Direct Coupled Wave Removal for GPR Data Based on SVD in the Wavelet Domain

Dejun CHEN [1], Ao XIANG [1], Shasha XIONG [1], Lin WANG [1], Li GUO [2]

[1] School of Information Engineering, Wuhan University of Technology, Wuhan, 430079, China
[2] Dept. of Information Engineering, Wuhan Electric Power Technical College, Wuhan, 430079, China

872387122@qq.com, mrchendj@163.com

Submitted August 2, 2022 / Accepted November 3, 2022 / Online first November 11, 2022

Abstract. *This paper presents a new algorithm of the singular value decomposition (SVD) in the wavelet domain for ground penetrating radar (GPR) to remove direct coupled waves. In fact, direct coupled waves commonly disturb the reflecting waves from underground targets. Besides, the amplitude and energy of direct coupled waves are large, which reduces the resolution of the images to the targets and adversely affects the subsequent image interpretation work. The GPR signal is decomposed into several levels by Wavelet to obtain approximation components and detailed components of each level. The information of targets is contained in big eigenvalues of detail components, while the direct coupled waves are contained in small ones. Therefore, the SVD in the wavelet domain can reduce the misjudgment of effective signals and improve the signal to noise ratio (SNR) of GPR signals. The simulated and field GPR data show that the SVD in the wavelet domain denoising method has better results for direct coupled wave removal than the traditional methods, which validates the effectiveness of the proposed denoising method.*

Keywords

Singular value decomposition, wavelet domain, ground penetrating radar, direct coupled waves, SNR

1. Introduction

Ground penetrating radar (GPR) is a geophysical exploration method that uses high frequency (1 MHz–10 GHz) electromagnetic waves to non-destructively detect invisible targets in the ground. With the advantages of simple operation, high resolution, and strong anti-interference capability, the GPR technology has been widely used in tunnel lining detection [1], [2], geological surveys [3], pipeline detection [4], [5], and many other fields. In the process of exploration, in order to maintain more reflected wave characteristics of targets, the GPR generally uses broadband to record. However, while collecting effective wave data, various interference signals such as noise and clutter will also be recorded in the original GPR data. In order to improve the accuracy of data interpretation, it is necessary to filter the original radar data and understand the effective echo characteristics of underground targets, which is of great significance to improve the level of data interpretation.

The echoes received from the GPR mainly include effective echoes of targets, direct coupled waves, and noise. Directly coupled waves have the characteristics of strong correlation, high noise intensity, and high energy, which is easy to cause the shallow target signals to be submerged. In addition, noise is mainly a non-smooth random signal, and its frequency is usually a function of time depth, so clutter suppression can reduce the false positive rate of deep target object recognition. At present, the processing methods of GPR noise mainly start from the time domain or frequency domain at home and abroad and use conventional sliding window filtering, frequency bandpass filtering, etc. These methods are often difficult to achieve ideal results, and cannot filter out some specific signal characteristics of GPR signals well. In order to solve the problem that the existing algorithms are not effective for GPR clutter suppressing, scholars at home and abroad have done a lot of research work. GPR denoising algorithms mainly include frequency filtering [6], fast independent component analysis (FastICA) [7], empirical mode decomposition (EMD) [8], neural network [9], singular value decomposition (SVD) [10], wavelet transform (WT) [11], KL transform [12].

The wavelet transform is independent of the smoothing factor in the signal, so it has distinct advantages in the analysis of complex non- stationary time series signals in both the time and frequency domains [13]. WT takes wavelet multi-scale analysis and fractal scale invariance, which have important applications in signal singularity and image processing [14], [15]. However, when different signals have different characteristics, similar wavelet functions require to be carefully selected. At present, Wu [16] proposed a denoising method based on wavelet transform to suppress random noise in GPR data. A 3-D wavelet denoising algorithm was proposed to remove direct coupled wave. It choosed a proper 2-D wavelet as the basic function and takes suitable wavelet scale to achieve this [17]. SVD is a useful method

DOI: 10.13164/re.2022.0564

to decompose the GPR data for final reconstruction of GPR signals by spectral analysis [18]. Downs [19] used SVD-filtering to remove direct coupled waves generated by the presence of very shallow objects, which preserves higher-order eigenimages. Liu [20] applied SVD method to eliminate random noise and direct coupled waves from the GPR signals. By comparing the SVD denoising method, wavelet threshold denoising method, and bandpass filtering method on noisy synthetic data and field data, the SVD method can eliminate random noise and direct waves in GPR data effectively and validly to improve the signal to noise ratio (SNR) and makes the effectively reflected signal clearer. SVD can also be used as a supplementary method to suppress random noise. Xue [21] presented a method based on SVD of a window-length-optimized Hankel matrix. SVD is applied to decompose and reconstruct the Hankel matrix of the original GPR data by singular values corresponding to effective signals, which are used to suppress noise. But he didn't show enough GPR models to demonstrate this. Gao [22] showed that wavelet domain KL is a effective denoising method by showing enough synthetic models. But he didn't compare with other methods and show field data.

Considering the strong correlation between direct coupled wave signals and the non-stationary characteristics of noise signals, a filtering method for the SVD in the wavelet domain of GPR signals is proposed through the fusion design of the two algorithms based on the suppression ability of the SVD on correlated signals and the time-frequency analysis ability of wavelet transform. Compared with the wavelet-domain KL transform, SVD, wavelet transform, and KL, the SVD in the wavelet domain method has a stronger denoising capability and less disturbance to the reflected signal of the target body. Finally, the results based on simulated and field GPR data validate the effectiveness of the proposed denoising method.

2. The SVD in the Wavelet Domain Denoising Method

2.1 Selection of Wavelet Function

Stationary signals are often filtered in a way that is considered in terms of frequency. Fourier transform is the basic theory of frequency filtering, which is used to reflect the overall characteristics of signals in the time domain. Although Fourier analysis is completely accurate in the frequency domain, it cannot provide any information on the local time band, that is, it cannot provide any specific and accurate time information. As the amplitude of the GPR echo signal changes with time, it is clear that the signal is not a stationary signal, so the Fourier transform cannot be used to filter noise in the GPR echo signal.

The wavelet transform has the property of multi-resolution analysis, which can effectively overcome the shortcomings of the Fourier transform lacking temporal localization. It is able to give information about the frequency of the signal while giving the moment when the frequency occurred, and dynamically adjusts the time and frequency domain windows according to the shape of the signal. Therefore, the wavelet transform method is widely used in the field of time-frequency analysis.

Different from the Fourier transform, which uses the sine and cosine functions as basic functions, the wavelet transform uses the wavelet function as the basic function. In theory, any function of $L^2(R)$ function space can be used as a wavelet function.The function of square integrable space can be decomposed orthogonally like vector space, and its mathematical expression is:

$$f(t) = \sum_{i=1}^{\infty} c_i g_i(t) \tag{1}$$

where $g_i(t)$ is the standard orthonormal basis; c_i is the projection of the signal on the basis function, which gives the information associated with the basis function $g_i(t)$:

$$c_i =< f(t), g_i(t) >= \int_{-\infty}^{+\infty} f(t) g_i^*(t) \mathrm{d}t. \tag{2}$$

For the wavelet transform denoising algorithm, it is crucial that how to appropriately choose a wavelet function. In addition, the more similar a wavelet function is to a signal waveform to be processed, the better the denoising effect [23]. It can be seen that the DB family wavelet function is similar to the GPR echo signal, as shown in Fig. 1.

Except for $N = 1$, DBN is not symmetrical (i.e. non-linear in phase), resulting in phase distortion when the signal is decomposed and reconstructed. As the wavelet order increases, the vanishing moments increase and the smoothness becomes better. At the same time, the amount of computation is greatly increased and the real-time performance becomes worse. If the SNR are similar, the wavelet function corresponding to the smaller N value is chosen as the basis function, which is beneficial for data compression and noise suppression. The wavelet function is selected from DB1 to DB20, and the SNR is used as the evaluation index to evaluate the analysis. Take the SNR result of the above 40$^{\text{th}}$ single-channel waveform for example, as is shown in Fig. 2. We can see that the SNR is the highest when $N = 4$ or 7, so DB4 wavelet is chosen as the wavelet function for the proposed algorithm.

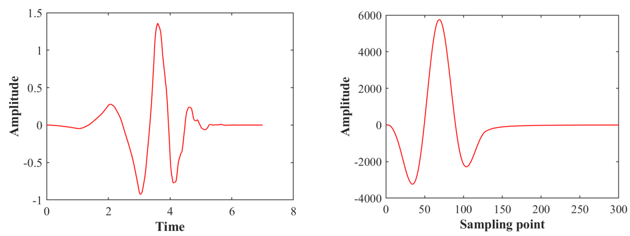

(a) (b)

Fig. 1. Comparison of DB family wavelet function and GPR single-channel signal. (a) DB family wavelet function, (b) The 40$^{\text{th}}$ single-channel waveform.

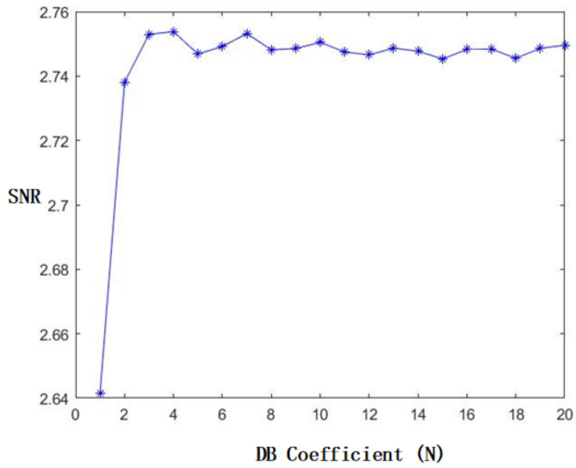

Fig. 2. Comparison of different DB wavelet decompositions.

2.2 Singular Value Decomposition

The GPR echo signal F mainly generated by effective echoes f from the targets, direct coupled waves g and noise clutter s is described by [23]:

$$F = f + g + s. \tag{3}$$

Assuming that the echo signal $\mathbf{F}$ denotes a $m \times n$ matrix, m denotes the number of sampling points of a single channel and n denotes the total number of channels of the signal, there must exist orthogonal matrices $\mathbf{U} = [u_1, u_2, \ldots, u_m] \in \mathbf{R}^{m\times m}$ and $\mathbf{V} = [v_1, v_2, \ldots, v_n] \in \mathbf{R}^{n\times n}$ satisfying:

$$\mathbf{U}^{\mathrm{T}}\mathbf{\Sigma}\mathbf{V} = \begin{pmatrix} \Sigma_r & 0 \\ 0 & 0 \end{pmatrix} \tag{4}$$

where $\Sigma_r = \operatorname{diag}(\sigma_1, \sigma_2, \ldots, \sigma_r)$, the diagonal component σ_i is the non-zero singular value in a non-increasing order (i.e. $\sigma_1 \geq \sigma_2 \geq \cdots \geq \sigma_r$) and $\mathbf{I}$ is the unit matrix. Let $\mathbf{U}$ and $\mathbf{V}$ be the left singular and right singular matrices, respectively, then, equation (3) can be rewritten as:

$$\mathbf{F} = \mathbf{U}\mathbf{\Sigma}\mathbf{V}^{\mathrm{T}} = \sum_{i=1}^{n} \sigma_i \mathbf{u}_i \mathbf{v}_i^{\mathrm{T}} \tag{5}$$

where the vector $\mathbf{u}_i$ and $\mathbf{v}_i$ are the left and right singular vectors of the matrix $\mathbf{F}$, respectively, $\mathbf{u}_i\mathbf{v}_i^{\mathrm{T}}$ is an adapted basis and σ_i is its coefficients. From (5), the components are statistically theoretically uncorrelated, indicating that the energy is concentrated in the vector matched by the larger eigenvalues. Therefore, the direct coupled wave can be filtered out by selecting the appropriate term and setting it to zero.

2.3 SVD in the Wavelet Domain

In theory, the SVD can effectively remove the components of direct coupled waves from the GPR signal, but in practice, the accuracy of its recognition of target echoes and clutter is not high. Specifically, in the shallow region, the target echo signal is easily misjudged as direct coupled waves to be removed, while in the deep region, the target echo signal is easily misjudged as clutter to be suppressed. Therefore, the SVD is not suitable for the global decomposition of GPR signals. What′s more, the core idea of the wavelet thresholding algorithm is to decompose the signal in the time-frequency domain to identify and filter noise, but it does not achieve ideal results for the non-smooth random signal of GPR. On the one hand, its accuracy in identifying target echoes and clutter is not very high, and it is not effective in filtering out direct coupled waves. On the other hand, the selection of the threshold value is very demanding, that is, too high cannot effectively filter out the noise, and too low tends to filter out the effective echo signal.

Therefore, we propose a new denoising algorithm based on SVD in the wavelet domain, which transforms the object of singular value transformation from the original complete echo signal to the approximate and detailed components obtained from wavelet multilayer decomposition, reducing the misjudgement of valid signals by the SVD and wavelet thresholding methods and improving the filtering accuracy. The SVD in the wavelet domain denoising process is shown in Fig. 3.

Step 1: Wavelet N-layer decomposition of the GPR signal $\mathbf{F}$ to obtain the approximate component A_N and the detail components of each layer D_i, $i = 1, 2, \cdots, N$.

Step 2: Perform SVD and inversion of all components obtained in Step 1 to obtain the approximate component W_{N+1} and the detail components of each layer W_j, $i = 1, 2, \cdots, N$.

Step 3: Wavelet N-layer reconstruction is performed based on all the components obtained from the inverse transform of Step 2, resulting in a filtered echo signal based on SVD in the wavelet domain.

Since direct coupled waves have strong correlation, their energy is basically concentrated in the first k $(k < r)$ larger eigenvalues. Firstly, the matrix $\mathbf{F}$ is constructed and decomposed using the SVD method. Secondly, the $\mathbf{U}$ and $\mathbf{V}$ components corresponding to the first k eigenvalues are set to zero, making the noise components are removed from the matrix $\mathbf{F}$. Finally, we obtain the target echo signal after filtering the direct coupled wave and random noise.

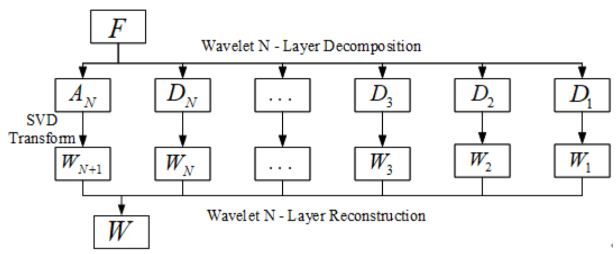

Fig. 3. The denoising process of SVD in the wavelet domain.

2.4 Performance Evaluation

In order to demonstrate that the SVD in the domain denoising method performs well, signal to noise ratio (SNR), root mean square error (RMSE), and normalization cross correlation (NCC) are used to compare and analyze the GPR data before and after direct coupled wave removal. They are defined below:

$$SNR = 10 \times \lg\left(g^2/(g-f)^2\right), \tag{6}$$

$$RMSE = \sqrt{\frac{1}{mn}\sum_{i=1}^{m}\sum_{j=1}^{n}\left(g_{j,k}-f_{j,k}\right)^2}, \tag{7}$$

$$NCC = \frac{\sum\limits_{i=1}^{m}\sum\limits_{j=1}^{n} g_{j,k}f_{j,k}}{\sqrt{\left(\sum\limits_{i=1}^{m}\sum\limits_{j=1}^{n} g_{j,k}f_{j,k}\right)\times\left(\sum\limits_{i=1}^{m}\sum\limits_{j=1}^{n} f_{j,k}g_{j,k}\right)}} \tag{8}$$

where $m \times n$ describes the size of GPR data. g is the original GPR data. f is the GPR data after removing direct coupled wave. These can be considered as indicators of the performance of the filtering method applied by identifying the technique (or the parameters) which results in the highest SNR and NCC with the lowest possible RMSE.

3. Application to GPR Simulation Data

3.1 Simulation Conditions

GPR applies high-frequency pulsed electromagnetic waves emitted by an antenna to detect target objects. The GPR system includes the transmitting signal part, the collecting signal part, and the signal processing part. The main structure and mode of the GPR are shown in Fig. 4, which includes the hardware equipment: host computer, transmitting antenna, transmitter, receiving antenna, receiver and computer. Firstly, the GPR transmits electromagnetic waves to the ground through the transmitting antenna, which are reflected, refracted, and projected on the ground. Then, the signals are received by the receiving antenna, and processed on a computer, which converts the collected electromagnetic signals into digital signals for processing.

The host computer is responsible for setting the frequency of the electromagnetic wave signal, the power of the machine, and other parameters. The electromagnetic wave signal is generated by the transmitting antenna. When the electromagnetic wave reaches the intersection of air and ground, part of signals will be reflected to be received by the receiving antenna, which is called direct waves. Signals from the transmitting antenna and then directly received by the receiving antenna is called a coupled wave. Direct waves and coupled waves belong to direct coupled waves. There is also a part of signals that reaches the target and then reflects is called the target signal. When the target echo signal reaches the receiver, it needs to be sampled and processed by the radar receiver, and then transmitted to the control module and processing module in the system, and finally, the original GPR signal is obtained through data processing.

FDTD can be able to completely simulate the process of GPR electromagnetic wave propagation in a computer. An important area of FDTD research is the design of an absorbing boundary condition that produces good results with small numerical reflections. The effectiveness of the absorption boundary condition is assessed by the size of the computational volume and the volume of the computational local area. The smaller the computational volume and the volume of the local area, the better the absorption boundary condition. Absorption boundary conditions can be divided into natural and forced boundaries, with natural boundaries being computationally simple but less effective. A representative example of a forced boundary is the perfectly matched layer (PML). This is where the electromagnetic wave arrives at the boundary and is first decomposed in all directions and different loss factors are applied to the components in different directions.

Finite difference time domain is the most common scientific modelling method, which works by replacing the first-order partial quotient in time and space with a central difference quotient, and then obtaining the distribution of the electromagnetic field by modelling the propagation process of electromagnetic waves in the time domain [24]. In this paper, Matlab is chosen as the application tool of the FDTD method to simulate the detection scenario and detection process of GPR data.

3.2 Observed Signals of Cavity Disease Model

Experiments performed on simulation data demonstrate that the superiority of SVD in the wavelet domain method over conventional filtering methods in terms of random noise suppression and direct wave removal. The dataset can be used to evaluate SVD in the wavelet domain method and also to establish evaluation criteria for field GPR data.

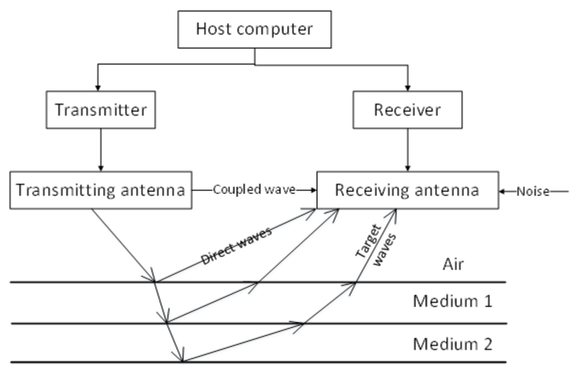

Fig. 4. Principle of GPR model.

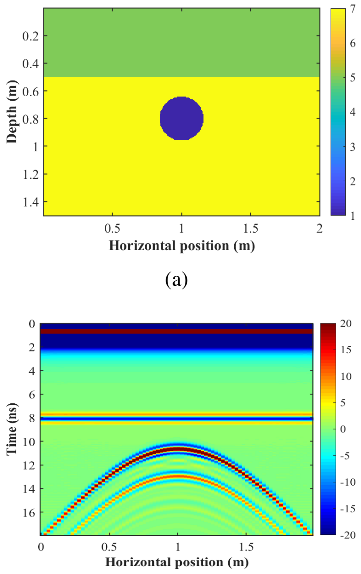

(a)

(b)

Fig. 5. (a) Subsurface model used to generate GPR data. (b) The GPR-data profile.

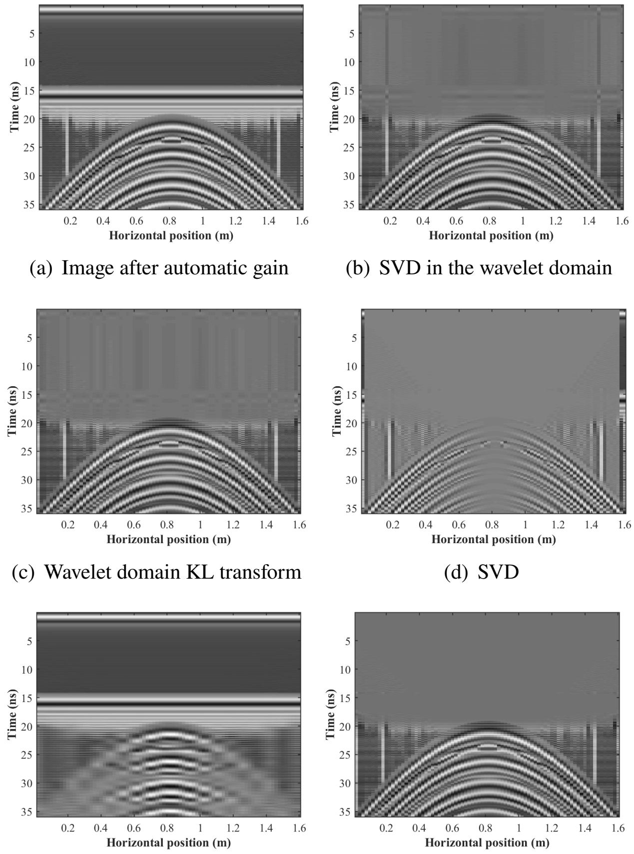

(a) Image after automatic gain (b) SVD in the wavelet domain

(c) Wavelet domain KL transform (d) SVD

(e) Wavelet transform (f) KL

Fig. 6. Results of direct wave arrivals removal for GPR simulation data.

In order to be closer to the field data, we simulated the parameters of the GPR equipment as much as possible. Specifically, the GPR pulse frequency is 900 MHz, 80 channels of single-channel echo data, and each consists of 1000 sampling points. The sampling time is 2 ns, and the channel interval is 0.2 m. In this paper, we have constructed a geological structure model with two layers. The tested model is shown in Fig. 5. The model length and depth are 1.6 m and 1.2 m respectively. The first layer is the pavement layer with a thickness of 0.4 m, which is composed of asphalt with the relative dielectric constant of 5 and conductivity of 0.01 S/m. The second floor is the road subgrade, mainly composed of soil or gravel with the relative dielectric constant of 6 and a conductivity of 0.1 S/m, with a thickness of 0.8 m. According to Fig. 5, it can be seen that the energy of the direct wave is stronger, and by contrast the energy of effective reflecting wave is weak.

3.3 Simulation Data Results

In order to demonstrate the superiority of the SVD in the wavelet domain method for GPR data, the wavelet domain KL, SVD, wavelet transform, KL transform filter method are used to remove direct coupled wave for comparison. As shown in Fig. 6(a), the direct coupled wave is mainly between 15–18 ns. From a subjective point of view, the SVD in the wavelet domain filtering algorithm remove the direct coupled wave better, and there is no obvious clutter, which does not affect the target echo signal. Although the wavelet domain KL filtering algorithm filter out the direct coupled wave, obvious clutter greatly affects the quality of the GPR echo image. From Fig. 7(d), we can see that the direct coupled wave can be removed completely, but does not distinguish well between background and target, resulting in a partially missing target echo. From Fig. 7(e), wavelet transform cannot remove the direct coupled wave, but it greatly suppress random noise. But when the interface between different layers is undulating, wavelet transform may cause false reflector in the profile. From Fig. 7(f), it can be seen that KL method effectively removes direct coupled waves from the GPR profile by choosing a suitable k-value. Comparing Figs. 7(b) and (c), we can know that the SVD in the wavelet domain can remove direct coupled waves and eliminate random noise from the GPR profile without losing useful information. Comparing Figs. 7(b) and (e), we can know that SVD in the wavelet domain can not only remove the direct coupled wave from the GPR profile, but also can eliminate the diffraction wave due to boundary effect.

Figure 7 shows the result of the 40$^{\text{th}}$ single channel waveform of gain GPR echo signal of the test model. The three filtering algorithms, including SVD in the wavelet domain, wavelet domain KL transform and KL, basically did not cause any disturbance to the amplitude and phase of the cavity echo signals, and the cavity area echo signals are basically the same as before filtering, proving that the three methods ensure that the signal amplitude of the target reflection area does not change. According to the waveform diagram, the amplitude residuals after filtering the direct coupled waves by the wavelet domain are significantly higher than SVD in the wavelet domain between sampling points 0 and 100. Between sampling points 100 and 350, the wavelet domain

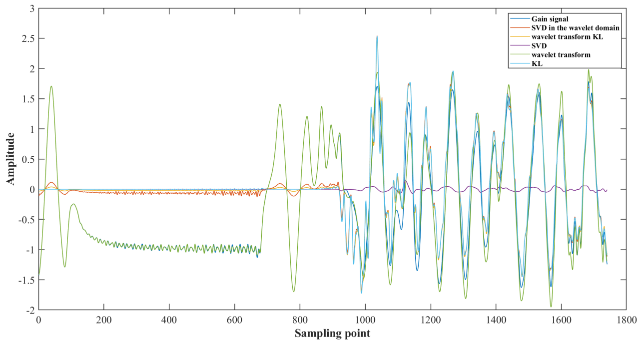

Fig. 7. Comparison of 40th single-channel signal wave before and after direct wave arrivals removal.

Methods	SNR	RMSE	NCC
SVD in the wavelet domain	3.2829	0.0149	0.7283
Wavelet domain KL [22]	3.1151	0.0152	0.7159
SVD [10]	1.5964	0.1372	0.5257
Wavelet transform [11]	1.1953	0.1049	0.8642
KL [12]	3.0257	0.0384	0.7194

Tab. 1. The SNR, RMSE, NCC of SVD in the wavelet domain, wavelet domain KL, SVD, wavelet transform and KL for simulation data.

KL filtering algorithm suppresses the amplitude of the waveform in this section to zero which also indicates that the wavelet domain KL filtering algorithm does not select the direct coupled wave portion accurately enough and filters out other valid reflected waves, while SVD in the wavelet domain filtering algorithm does not filter out this segment of the echo signal waveform and corrects it to zero, completely ensuring that only the direct coupled wave is filtered out, proving the superiority of SVD in the wavelet domain filtering algorithm proposed in this paper. Between sampling points 600 and 100, wavelet domain may cause false reflector in the profile. On the contrary, SVD in the wavelet domain don't cause false reflector. From the results of SVD denoising, it is clear that direct SVD decomposition cannot effectively separate the target signal from the background signal without selecting suitable singular values.

Table 1 shows that the SVD in the wavelet domain filtering algorithm outperforms the wavelet domain KL filtering algorithm in terms of SNR, RMSE and NCC. In addition, the SVD in the wavelet domain can better preserve the integrity of the signal, so that the denoised signal still retains the signal characteristics from underground targets. The closer the NCC is to 1, the more similar it represents to the original image. Wavelet transform has the highest NCC value which is shown in Tab. 1. The main reason for this is the strong coherence and high energy of direct coupled waves, resulting in the highest NCC value for the worst denoising effect. We only use the NCC as an auxiliary evaluation metric. Under the premise of better removal of direct coupled waves, the value of NCC is used to objectively judge whether the denoising is excessive or not. There's no doubt that wavelet transform does not remove direct coupled waves very well. Although the KL filtering algorithm is similar to SVD in the wavelet domain in terms of SNR, RMSE and NCC, it disrupts near-surface target signals. The processing results shows that the SVD in the wavelet domain filtering algorithm has higher accuracy than the wavelet domain KL filtering algorithm, SVD, the wavelet domain, KL, which are popularly used now. What's more, it can also remove the diffraction wave due to boundary effect.

4. Application to Field GPR Data

4.1 Measurement Setup

Based on field GPR data, the filtering performance of the SVD in the wavelet domain is analyzed. Taking the concrete structural masonry experimental wall of the Iron Academy of Sciences as the research object, the Italian RIS-type GPR and 900 MHz shielded antenna were used for inspection. According to echo images, it can be judged that the second lining rebar is mainly distributed in the time depth range of 5–10 ns, while the direct coupled wave is mainly concentrated in the time depth of 5 ns. The rebar echo is closer to the direct coupled wave, which lead to a small amount of echo signal is covered.

The experimental wall is 50 cm thick, 1.5 m high and 15 m long. It is divided into a reinforced layer and an unreinforced layer. There are 12 cavities in the unreinforced layer, 4 in each height section. In the reinforced layer, the diameter of the reinforcement is 22 mm and the spacing is 25 cm. The distance from the wall surface is divided into three layers: 25 cm, 15 cm and 5 cm. The types of cavities are 5 cm × 30 cm, 10 cm × 30 cm and 15 cm × 30 cm. The radar has 512 sampling points, a time window of 40 ns and a channel spacing of 4 mm.

4.2 Field GPR Data Results

In order to verify the practicality of wavelet singular value filtering, this section takes the field data of GPR detection in Italy as an example. After gaining the original GPR echo data, the SVD in the wavelet domain filtering algorithm is used to process the direct coupled waves, and the results are shown in Fig. 8. From Fig. 8(d), we can see that there is no signal on the image, which indicates that the SVD denoising algorithm cannot be applied to the field data. From Fig. 8(e), wavelet transform does not have any effect, while KL denoising method performed very well. The processing results shows the SVD in the wavelet domain method is suitable for GPR field data denoising. It not only removes diffracted waves due to boundary effects, but also effectively removes the direct coupled wave from the GPR profile without destroying the near-surface target signal.

As can be seen from Fig. 8, the SVD in the wavelet domain filtering algorithm filters out the direct coupled wave and makes the cavity disease area more prominent, which is more conducive to the operator's identification and observation, proving the practicality of the SVD in the wavelet domain filtering algorithm.

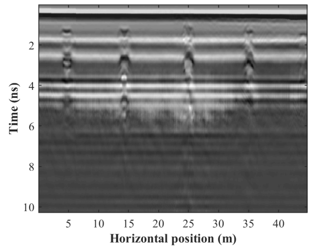

(a) Field GPR data after automatic gain

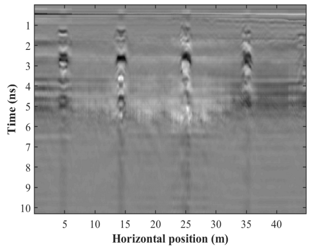

(b) SVD in the wavelet domain

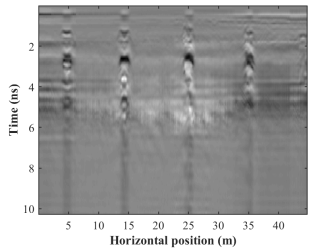

(c) Wavelet domain KL transform

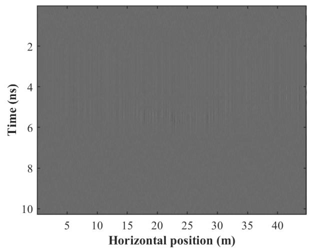

(d) SVD

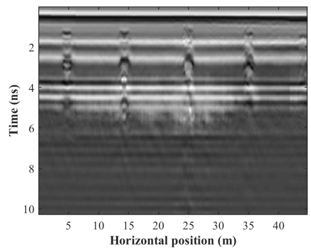

(e) Wavelet transform

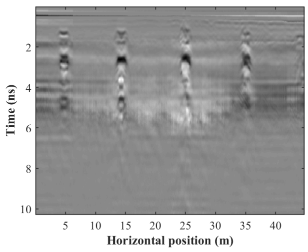

(f) KL

Fig. 8. Results of direct wave arrivals removal for field GPR data.

5. Conclusions

In this paper, we have proposed a SVD in the wavelet domain algorithm for GPR data to remove direct coupled waves. Experimental results demonstrated that our method consistently outperform the state-of-the-art methods across several challenging benchmarks (including wavelet domain KL transform). The three main contributions for performance improvement are vanishing moment of the wavelet system, wavelet N-layer reconstruction, singular value decomposition and its inverse transformations.

The processing results from the field measured data show that our method is more stable and convenient than the other denoising methods, which can remove direct coupled waves. The SVD in the wavelet domain not only removes diffracted waves due to boundary effects, but also effectively removes the direct coupled wave from the GPR profile without destroying the near-surface target signal. The improved SNR and accuracy in GPR data interpretation help to highlight the characteristics of abnormal bodies in GPR profiles. It is worth noting that the real geological structure is much more complex. We have only considered one category of cavity in two layers of geological conditions, and the applicability of the method needs to be improved.

Acknowledgments

This work was supported by the Chinese Academy of Railway Science Foundation Project (1951JJ5703).

References

[1] YAN, J., BO, W., ZHAO, X., et al. Application of ground penetrating radar in reservoir leakage detection in complex geological areas. *IOP Conference Series: Earth and Environmental Science*, 2021, vol. 706, no. 1, p. 1–9. DOI: 10.1088/1755-1315/706/1/012009

[2] WANG, S., LIU, G., JING, G., et al. State-of-the-art review of ground penetrating radar (GPR) applications for railway ballast inspection. *Sensors*, 2022, vol. 22, no. 7, p. 2450–2478. DOI: 10.3390/s22072450

[3] GHOZZI, R., LAHOUAR, S., SOUANI, C. FDTD-based sensitivity analysis of GPR acquisition parameters for accurate detection of buried cylindrical objects. *Electronics Letters*, 2022, vol. 58, no. 3, p. 118–120. DOI: 10.1049/ell2.12371

[4] VAUGHAN, C. J. Ground-penetrating radar surveys used in archaeological investigations. *Geophysics*, 1986, vol. 51, no. 3, p. 595–604. DOI: 10.1190/1.1442114

[5] BASILE, V., CARROZZO, M. T., NEGRI, S., et al. A ground-penetrating radar survey for archaeological investigations in an urban area (Lecce, Italy). *Journal of Applied Geophysics*, 2000, vol. 44, no. 1, p. 15–32. DOI: 10.1016/S0926-9851(99)00070-1

[6] WEI, X., ZHANG, Y. Interference removal for autofocusing of GPR data from RC bridge decks. *IEEE Journal of Selected Topics in Applied Earth Observations and Remote Sensing*, 2015, vol. 8, no. 3, p. 1145–1151. DOI: 10.1109/JSTARS.2015.2402211

[7] SALAZAR, A., SAFONT, G., VERGARA, L. Application of independent component analysis for evaluation of Ashlar masonry walls. In *International Work-Conference on Artificial Neural Networks (IWANN)*. Torremolinos-Malaga (Spain), 2011, p. 469–476. DOI: 10.1007/978-3-642-21498-1_59

[8] LI, J., LIU, C., ZENG, Z., et al. GPR signal denoising and target extraction with the CEEMD method. *IEEE Geoscience and Remote Sensing Letters*, 2015, vol. 12, no. 8, p. 1–5. DOI: 10.1109/LGRS.2015.2415736

[9] FENG, D., WANG, X., WANG, X. Deep convolutional denoising autoencoders with network structure optimization for the high-fidelity attenuation of random GPR noise. *Remote Sensing*, 2021, vol. 13, no. 9, p. 1–22. DOI: 10.3390/rs13091761

[10] MUZY, J. F., BACRY, E., ARNEODO, A. Multifractal formalism for fractal signals: The structure-function approach versus the wavelet-transform modulus-maxima method. *Physical Review E*, 1993, vol. 47, no. 2, p. 875–884. DOI: 10.1103/PhysRevE.47.875

[11] BAILI, J., LAHOUAR, S., HERGLI, M., et al. GPR signal de-noising by discrete wavelet transform. *NDT & E International*, 2009, vol. 42, no. 8, p. 696–703. DOI: 10.1016/j.ndteint.2009.06.003

[12] HUO, Z., WANG, M. The application of KL transform to remove direct wave in ground penetrating radar records. In *International Conference on Image and Graphics (ICIG)*. Chengdu (China), 2007, p. 133–138. DOI: 10.1109/ICIG.2007.173

[13] SONG, C., LU, Q., LIU, C., et al. Random noise de-noising and direct wave eliminating in ground penetrating radar signal using SVD method. In *International Conference on Ground Penetrating Radar (GPR)*. Hong Kong (China), 2016, p. 1–5. DOI: 10.1109/ICGPR.2016.7572636

[14] JIANG, Z., ZHOU, W., STANLEY, H. E. Multifractal cross wavelet analysis. *Fractals*, 2017, vol. 25, no. 6, p. 1–10. DOI: 10.1142/S0218348X17500542

[15] BACRY, E., MUZY, J. F., ARNEODO, A. Singularity spectrum of fractal signals from wavelet analysis: Exact results. *Journal of Statistical Physics*, 1993, vol. 70, no. 3, p. 635–674. DOI: 10.1007/BF01053588

[16] WU, Z., LIU, T., HUA, C. Wavelet threshold de-noising based on higher-order statistics in attenuating random noise. *SEG Technical Program Expanded Abstracts*, 2006, vol. 25, no. 1, p. 58–61. DOI: 10.1190/1.2370119

[17] SHI, X., YANG, Q. Suppressing the direct wave noise in GPR data via the 2-D physical wavelet frame. In *Proceedings of the International Conference on Transportation, Mechanical, and Electrical Engineering (TMEE)*. Changchun (China), 2011, p. 1161–1164. DOI: 10.1109/TMEE.2011.6199411

[18] JIN, L., CHEN, X. The combination of wavelet transform and nonlinear filtering for time-lapse seismic difference analysis. *SEG Technical Program Expanded Abstracts*, 2008, vol. 27, no. 1, p. 3214–3218. DOI: 10.1190/1.3064013

[19] DOWNS, C., JAZAYERI, S. Resolution enhancement of deconvolved ground penetrating radar images using singular value decomposition. *Journal of Applied Geophysics*, 2021, vol. 193, p. 1–18. DOI: 10.1016/j.jappgeo.2021.104401

[20] LIU, C., SONG, C., LU, Q. Random noise de-noising and direct wave eliminating based on SVD method for ground penetrating radar signals. *Journal of Applied Geophysics*, 2017, vol. 144, no. 3, p. 125–133. DOI: 10.1016/j.jappgeo.2017.07.007

[21] XUE, W., LUO, Y., YANG, Y., et al. Noise suppression for GPR data based on SVD of window-length-optimized Hankel matrix. *Sensors*, 2019, vol. 19, no. 17, p. 1–25. DOI: 10.3390/s19173807

[22] GAO, Y. T., XU, J. Geological radar signal processing techniques based on wavelet domain KL transform. *Science Technology and Engineering*, 2018, vol. 18, no. 10, p. 161–166, (in Chinese).

[23] WU, X., YAN, F., ZENG, R., et al. Research on ground-penetrating radar clutter suppression based on wavelet transform and K-SVD. *Journal of Hebei University of Science and Technology*, 2021, vol. 42, no. 2, p. 111–118, (in Chinese).

[24] FENG, D., DAI, Q., HE, J., et al. Finite-difference time-domain implementation of ground-penetrating radar GPR orthorectified simulation. *Advances in Geophysics*, 2006, vol. 2, p. 630–636, (in Chinese).

About the Authors . . .

Dejun CHEN was born in 1964. He received his D.E. in 2003. His research interests include complex system modeling, distributed decision support systems, embedded systems.

Ao XIANG was born in 1997. She received her M.Sc. in 2022. Her research interests include signal processing and image processing.

Shasha XIONG (corresponding author) was born in 1997. Her research interests include signal processing and image processing.

Lin WANG was born in 1972. Her research interests include fiber optic communications and electromagnetic fields and microwaves.

Li GUO was born in 1981. Her research interests include computer simulation, computer networks and communication.